Advance Sustainable Science, Engineering and Technology (ASSET)
Vol. 8, No.4, October 2026, pp. 02604026-01 ~ 02604026-013
ISSN: 2715-4211 DOI: https://doi.org/10.26877/asset.v8i4.3858

A Sustainable Computational Framework for Breast Cancer Screening: Optimizing High-Dimensional Feature Spaces via MVP-PCA for Resource-Constrained Environments

Etika Kartikadarma*, Ahmad Zainul Fanani, Pujiono, Affandy

Faculty of Computer Science, Dian Nuswantoro University, Jl. Imam Bonjol No.207, Semarang 50131, Central Java, Indonesia

*etika.kartikadarma@dsn.dinus.ac.id

Abstract. The rapid integration of Electronic Health Records (EHR) demands the efficient processing of high-resolution medical images. However, deep learning architectures applied to mammography classification often produce massive, high-dimensional feature spaces susceptible to the curse of dimensionality and anatomical noise. Furthermore, conventional dimensionality reduction approaches tend to cause over-reduction, which destroys crucial microcalcification textures. To address these challenges, this study proposes a CPU-efficient hybrid dimensionality reduction framework integrating Mean Vector Projection (MVP) and Principal Component Analysis (PCA) on features extracted by SqueezeNet. The MVP layer acts as a crucial pre-conditioner to stabilize intra-class variance before PCA decomposition. Experimental results demonstrate that the proposed MVP-PCA framework successfully linearizes the feature space and achieves an extreme compression rate of 99.11%, reducing 264,702 features to 2,355 essential components. The peak accuracy reaches 97.58% with a minimal False Negative rate (2 cases), providing a sustainable diagnostic solution for healthcare facilities with limited technological resources.

Keywords: Breast Cancer Classification, Dimensionality Reduction, Mean Vector Projection, Principal Component Analysis, SqueezeNet

(Received 2026-05-21, Revised 2026-07-20, Accepted 2026-08-03, Available Online by 2026-08-29)

1. Introduction

The global transition toward digital-first healthcare ecosystems through Electronic Health Records (EHR) has transformed clinical workflows [1], [2], driven by an exponential surge in diagnostic imaging data [3]. However, the massive volume of high-resolution visual data generated daily places an unprecedented computational burden on radiology infrastructures [4]. While the Digital Imaging and

Communications in Medicine (DICOM) standard is indispensable for data exchange [5], [6], the sheer scale of these repositories presents formidable challenges for rapid data retrieval, making high-dimensional datasets a significant technological bottleneck for AI integration [7].

Convolutional Neural Networks (CNNs) have emerged as the gold standard for medical image classification due to their proficiency in autonomous feature extraction [8, 9]. These architectures excel at identifying complex pathological patterns that may be invisible to the human eye [10]. However, as deep learning models increase in depth and complexity to capture finer details, they often project data into an excessively high-dimensional feature space [11]. This phenomenon triggers the "curse of dimensionality," where the presence of anatomical noise and redundant features can obscure the actual diagnostic signal and degrade the performance of predictive models [12].

Furthermore, the deployment of sophisticated deep learning models typically necessitates high-performance hardware, such as GPU clusters, which consume significant energy and require substantial financial investment [13], [14]. This dependency creates a technological divide, limiting the accessibility of advanced AI diagnostics in resource-constrained clinical settings [15]. Consequently, there is an urgent need for sustainable and computationally efficient feature engineering techniques that can maintain high diagnostic precision while operating effectively on standard CPU-based infrastructures [16].

To address these limitations, conventional dimensionality reduction methods like PCA and LDA are widely utilized for data compression [17- 20]. However, their effectiveness is often hindered by the non-linear distribution of raw CNN features [21], [22]. To overcome this limitation, several nonlinear dimensionality reduction techniques, including Kernel PCA [23] and deep feature compression methods [24], have been introduced to better preserve complex feature relationships. Although improve feature representation, they incur higher computational costs, increased memory requirements, or additional trainable parameters, making them less suitable for resource-constrained environments. In lightweight CNN architectures, most of the work is still aimed at optimizing network parameters rather than improving the statistical structure of the feature space extracted before dimensionality reduction [25].

Motivated by this gap, this study proposes a sustainable hybrid dimensionality reduction framework that combines the lightweight SqueezeNet architecture with a Mean Vector Projection (MVP) preprocessing stage before PCA. The framework utilizes SqueezeNet, a lightweight CNN architecture optimized for parameter efficiency [26]. Instead of replacing PCA with a more complex nonlinear alternative, the proposed MVP conditions the extracted feature space through global mean centering and class-wise feature alignment, aiming to reduce irrelevant variance and improve feature organization before covariance-based projection. This strategy preserves the computational efficiency and interpretability of linear dimensionality reduction while enhancing feature separability for breast cancer classification in resource-constrained healthcare environments.

The main contributions of this study are threefold. First, we propose an MVP-based feature-space conditioning stage prior to PCA to improve the statistical organization of deep CNN features before covariance-based projection. Second, we integrate the proposed MVP-PCA framework with the lightweight SqueezeNet architecture to achieve computationally efficient breast cancer classification. Third, we demonstrate that the proposed framework preserves high diagnostic performance while substantially reducing feature dimensionality, making it suitable for resource-constrained healthcare environments.

2. Methods

Figure 1 illustrates the proposed framework, including preprocessing, SqueezeNet feature extraction, MVP-PCA dimensionality reduction, classification, and evaluation. Two pipelines are evaluated: P1 uses LDA as the final classifier, while P2 applies LDA for both reduction and classification. Experiments are conducted under CPU-based settings using stratified patient-wise data splitting to ensure fair and realistic evaluation.

2.1. Datasets and Preprocessing

This study uses the RSNA Screening Mammography Breast Cancer Detection dataset [27], containing malignant (1,158) and benign (53,548) mammographic images with standard CC and MLO views. A stratified patient-wise split was applied to prevent data leakage and patient-specific bias [28]. Raw DICOM images were converted to 8-bit grayscale PNG [27], resized and downsampled to 224×224 pixels for feature extraction [29], and grayscale channels were replicated into three-channel RGB format to meet the input requirements of the pre-trained architecture.

2.2. Lightweight Feature Extraction via SqueezeNet

To develop a CPU-efficient diagnostic framework, SqueezeNet was employed as the feature extraction backbone due to its parameter-efficient Fire Modules, which preserve robust feature representation while reducing computational overhead [26], [29]. After convolutional processing, Global Average Pooling (GAP) transforms the $(H \times W \times C)$ feature map into a one-dimensional vector for subsequent analysis. The overall workflow, including normalization, scaling, SqueezeNet processing, and GAP-based feature projection, is illustrated in Figure 2.

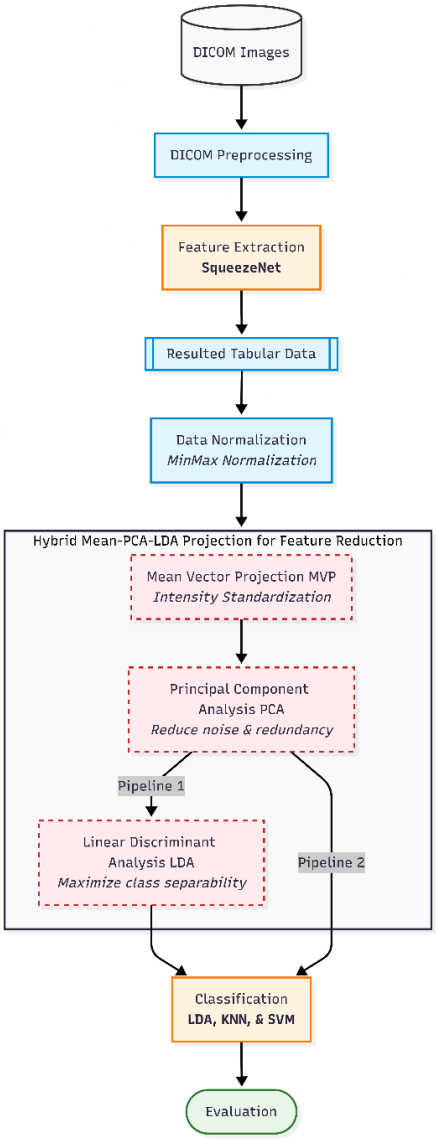

Figure 1. The **complete** workflow of the proposed hybrid dimensionality reduction framework, divided into Pipeline 1 (DirectClassification) and Pipeline 2 (Over-Reduction Analysis).

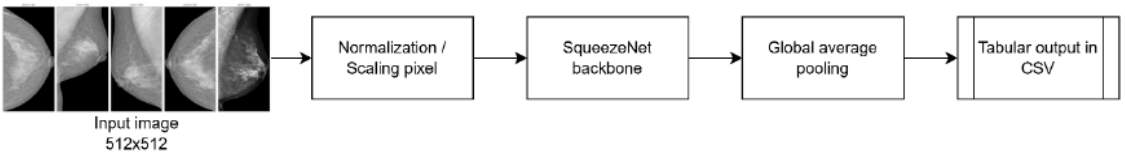

Figure 2. Feature extraction pipeline using SqueezeNet and Global Average Pooling (GAP) to transform normalized **mammography** images into one-dimensional feature vectors.

2.3. Proposed Hybrid Dimensionality Reduction (MVP-PCA)

Prior to applying dimensionality reduction techniques such as Principal Component Analysis (PCA) and Linear Discriminant Analysis (LDA), a Mean Vector Projection (MVP) preprocessing stage is introduced to stabilize the SqueezeNet-derived feature distribution through two sequential linear transformations: global mean centering to remove dataset bias, followed by class-wise mean alignment to reduce intra-class variability. This two-stage transformation produces a more structured and consistent feature space, improving its suitability for subsequent orthogonal dimensionality reduction methods such as PCA and LDA.

Before dimensionality reduction, the extracted deep features were first conditioned using the proposed Mean Vector Projection (MVP). Unlike conventional preprocessing that directly applies PCA to the extracted features, MVP performs sequential global and class-aware feature alignment to reduce irrelevant variance prior to covariance estimation. To avoid data leakage, all statistical parameters, including the global mean and class-wise means, were estimated exclusively from the training data and subsequently applied to transform both training and testing features.

Stage 1: Global Mean Centering

The global mean vector μ is first calculated to center the dataset distribution:

$$\mu = \frac{1}{n}\sum_{i=1}^{n} x_i \quad (1)$$

where μ denotes the global mean vector computed from all training feature vectors, and n represents the total number of training samples. The centered feature vector $x_i^{(1)}$ is then obtained by:

$$x_i^{(1)} = x_i - \mu \quad (2)$$

where x_i is the original feature vector and $x_i^{(1)}$ denotes the globally centered feature vector after mean subtraction. This step centers the feature distribution and facilitates covariance computation for PCA [30]. The global mean vector is computed exclusively from the training data and subsequently applied to transform both the training and testing feature sets, thereby preventing data leakage during preprocessing.

Stage 2: Class-wise Mean Alignment

To linearize the feature space, the features are adjusted based on their class-specific means μ_k :

$$\mu_k = \frac{1}{N_k}\sum_{i=1}^{N_k} x_i^{(1)}, \quad x_i^{(1)} \in C_k \quad (2)$$

where μ_k denotes the mean feature vector of class k, N_k is the number of training samples belonging to class k, and C_k represents the corresponding class. Furthermore, $x_i^{(2)}$denotes the MVP-conditioned feature vector after class-wise mean alignment.

$$x_i^{(2)} = x_i^{(1)} - \mu_{C(i)} \quad (3)$$

This class-wise mean alignment is performed to reduce intra-class variability while preserving inter-

class differences. The class mean is computed only from the training samples of each class and subsequently used to transform both training and testing features, ensuring that no information from the testing set contributes to the preprocessing stage.

Stage 3: PCA Refinement for Noise Reduction

PCA is applied to the stabilized features to eliminate redundant anatomical noise [31]. The eigenvalue problem is solved as:

$$Sv_k = \lambda_k v_k \quad (4)$$

where Sv_k denotes the covariance matrix of the MVP-conditioned features, λ_k is the eigenvalue corresponding to the k-th principal component, and $v_k$represents its associated eigenvector. The final projection is formulated as:

$$z_i = W_{PCA}^T(x_i - \mu), \quad \forall i = 1, \dots, N \quad (5)$$

where W_{PCA}^T denotes the projection matrix formed by the selected principal eigenvectors, and z_i is the reduced feature representation of sample i. Since the covariance matrix is estimated from the MVP-conditioned features, the resulting principal components are expected to better represent discriminative information than those obtained from the original feature distribution.

Stage 4: LDA Projection

For comparison purposes, an additional dimensionality reduction stage using Linear Discriminant Analysis (LDA) was incorporated in Pipeline 2. Unlike PCA, which preserves the directions of maximum variance, LDA seeks a projection that maximizes class separability according to Fisher's criterion [32], [33]:

$$W_{LDA} = \arg\max_W \frac{|W^T S_b W|}{|W^T S_w W|} \quad (6)$$

where S_b and S_w denote the between-class and within-class scatter matrices, respectively, and W_{LDA} represents the optimal projection matrix maximizing Fisher's discriminant criterion. The LDA projection serves as an additional benchmark to evaluate whether further supervised dimensionality reduction improves the representation obtained from MVP-PCA. In addition, KNN and SVM classifiers are employed to assess the generalization capability of the extracted features under different classification mechanisms.

To improve reproducibility, the overall implementation procedure of the proposed MVP-PCA framework is summarized in Algorithm 1. The algorithm describes the sequential process from feature preprocessing through dimensionality reduction before classification.

Algorithm 1. Proposed MVP-PCA Framework Pseudocode

```
Input :
    CNN feature matrix X
    Class labels Y

Output :
    Reduced feature matrix Z

1: Compute global mean μ
2: Center all feature vectors
       Xc = X − μ
3: For each class c
4:      Compute class mean μc
5:      Align all samples belonging to class c
6: End
```

```
7: Apply PCA on aligned features
8: Select principal components
9: Return reduced feature matrix Z
```

2.4. Classification Strategy and Evaluation Metrics

In the final stage, the transformed feature representations z are evaluated using LDA, KNN, and SVM to assess linear separability. LDA performs class assignment by maximizing the discriminant function as defined in Equation (13) [33], where Σ denotes the covariance matrix, μ_c represents the mean vector of class c, and $P_c$corresponds to the prior probability.

KNN serves as a non-parametric baseline using Euclidean proximity and majority voting among the nearest neighbors, while SVM is incorporated to further validate separability by constructing an optimal margin-based decision boundary [34], Both linear and Radial Basis Function (RBF) kernels are evaluated to determine whether the transformed feature space remains linearly structured or requires non-linear mapping. Performance is assessed using Accuracy, Precision, Recall (Sensitivity), F1-score, and confusion matrix analysis, with particular emphasis on minimizing false negatives (FN) in medical diagnosis [35].

$$g_c(z) = z^T\Sigma^{-1}\mu_c - \frac{1}{2}\mu_c^T\Sigma^{-1}\mu_c + \ln(P_c) \tag{7}$$

2.5. Experimental Setup and Hyperparameter Configuration

To ensure reproducibility, this section details the hyperparameter configuration and experimental protocol used throughout the study. Feature scaling was performed using Min-Max normalization, fitted exclusively on the training fold to prevent data leakage. For PCA, the number of components was set to 80 based on cumulative explained variance. LDA, when used as a dimensionality reducer (Pipeline 2), was constrained to C−1 components, where C denotes the number of classes. The KNN classifier used k=5 neighbors with Euclidean distance. For SVM, hyperparameters (C, kernel, gamma) were optimized via GridSearchCV over the grid {C: [0.1, 1, 10, 100], kernel: [linear, rbf], gamma: [scale, auto, 0.1, 1]}, using stratified 5-fold cross-validation on the full dataset prior to final evaluation. All experiments were conducted using Python 3.12 and scikit-learn 1.6.1, with a fixed random seed (123) to ensure reproducibility across runs. Final performance evaluation used independent stratified 5-fold cross-validation.

2.6. Computational Complexity Analysis

To quantitatively validate the framework's claim of CPU-efficiency, computational cost was measured for each combination of dimensionality reduction method and classifier across all cross-validation folds. Two metrics were recorded: (1) training time, measured as the wall-clock time required to fit the classifier on the transformed training features, and (2) inference time per sample, measured as the average wall-clock time required to generate a prediction for a single test instance, computed by dividing the total prediction time for a fold by the number of samples in that fold's test set.

Computational runtime was measured using Python's `time.perf_counter()`, which provides a high-resolution monotonic wall-clock timer suitable for benchmarking elapsed execution time. All experiments were conducted on a system equipped with an Intel Core i5-8250U CPU and 16 GB of RAM without GPU acceleration to emulate a resource-constrained clinical computing environment. To ensure a fair comparison among dimensionality reduction and classification methods, the one-time feature extraction stage using SqueezeNet was excluded from the runtime analysis, as it remains identical across all evaluated methods and does not affect the relative computational efficiency of the proposed framework.

3. Results and Discussion

3.1. Experimental Setup

The proposed MVP-PCA pipeline reduced the feature space from 264,702 dimensions to 2,355 principal components, corresponding to a dimensionality reduction of approximately 99.11%. This substantial compression indicates that the transformed feature space retains informative structure while significantly reducing computational complexity during classification.

3.2. Comparative Performance Analysis

To evaluate the specific contribution of the MVP layer, a rigorous ablation study was conducted. The performance comparison between the two experimental pipelines is summarized in (Table 1). The data reveals that the integration of MVP as a pre-conditioner for PCA (Pipeline 1) is the critical factor in achieving high accuracy.

Table 1. Classification Performance Comparison (Pipeline 1 vs. Pipeline 2)

Feature Reduction Stage	Pipeline Architecture	Final Classifier	Accuracy
PCA	Pipeline 1	LDA	0.8942
MVP + PCA	Pipeline 1	LDA	0.9758
PCA + LDA	Pipeline 2	LDA	0.8120
MVP + PCA + LDA	Pipeline 2	LDA	0.8315

As shown in Table 1, the highest accuracy (0.9758) is achieved by Pipeline 1 using MVP+PCA. These results show that applying MVP before PCA successfully improves classification performance compared to applying PCA alone. These findings demonstrate that conditioning the feature space prior to covariance-based projection allows PCA to retain more discriminative information, resulting in a more informative low-dimensional representation for subsequent classification. In contrast, Pipeline 2 exhibits a noticeable performance degradation to 0.8120 after the additional LDA reduction stage. Because LDA projects the data into a subspace with at most $C - 1$ dimensions, applying LDA after PCA substantially compresses the feature representation. This aggressive reduction likely removes informative variance that is still relevant for classification, explaining the lower predictive performance.

Figure 3 further supports this interpretation by illustrating the cross-validation accuracy distributions across all evaluated pipelines. The MVP-PCA pipeline demonstrates not only the highest median accuracy but also the narrowest interquartile range, indicating that the proposed preprocessing strategy produces more stable predictive performance across different validation folds.

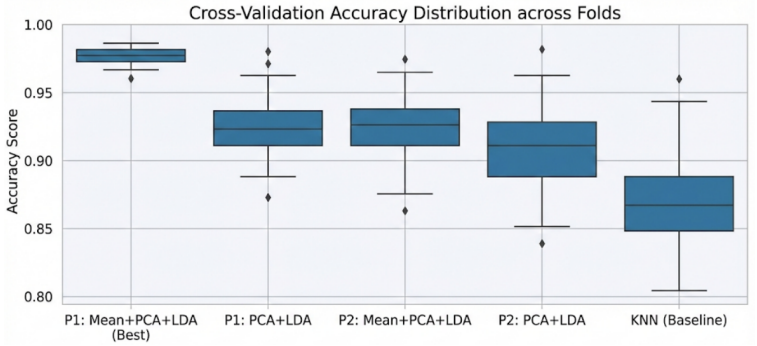

Figure 3. Cross-validation accuracy distribution across folds.

Overall, these findings indicate that the contribution of MVP does not lie in replacing PCA with a more sophisticated dimensionality reduction algorithm, but rather in conditioning the feature distribution before covariance estimation. This preprocessing step enables conventional linear projection to operate on a statistically better-organized feature space, providing improved predictive performance

without introducing additional optimization procedures or trainable parameters.

3.3. Computational Efficiency Analysis

To validate the framework's efficiency claims quantitatively, Table 2 summarizes the computational cost of each dimensionality reduction method paired with its best-performing classifier.

Table 2. Computational Complexity Comparison (Best Classifier per Method)

Feature Reduction	Reduction Time (s)	Best Classifier	Classifier Train Time (s)	Total Pipeline Time (s)	Inference Time/Sample (ms)
PCA	0.213	LDA	0.012	0.225	0.0037
MVP + PCA	0.179	LDA	0.017	0.196	0.0030
PCA + LDA	0.370	SVM (tuned)	0.003	0.372	0.0041
MVP + PCA + LDA	0.456	KNN	0.002	0.458	0.1220

Among all evaluated methods, the proposed MVP+PCA framework achieved the lowest overall computational cost, requiring only 0.196 s for the complete training pipeline, compared with 0.225 s for conventional PCA, 0.372 s for PCA+LDA, and 0.458 s for the complete MVP+PCA+LDA framework. Interestingly, the proposed method also exhibited a shorter feature reduction time (0.179 s) than standard PCA (0.213 s), suggesting that the MVP preprocessing stage effectively stabilizes the feature distribution prior to PCA, allowing the subsequent dimensionality reduction process to converge more efficiently despite the additional preprocessing step.

Inference efficiency further supports the suitability of the proposed framework for resource-constrained environments. MVP+PCA required only 0.0030 ms per sample, representing the fastest inference among all evaluated methods while maintaining competitive classification performance. In contrast, incorporating an additional LDA projection increased both the total pipeline time and inference latency, with the MVP+PCA+LDA configuration reaching 0.1220 ms per sample. These findings indicate that although additional supervised feature transformations may improve feature discrimination in certain cases, they introduce extra computational overhead. Consequently, the proposed MVP+PCA framework provides a more favorable balance between computational efficiency and classification capability, supporting its applicability for CPU-based medical image analysis where low runtime and minimal computational resources are essential.

3.4. Proof of Feature Linearization and Kernel Comparison

A core scientific objective of this study was to prove that the MVP layer successfully linearizes the feature space. This is validated by comparing the performance of Linear and Non-Linear kernels, as presented in (Table 3).

Table 3. Performance Comparison of SVM and LDA

Algorithm	Kernel/Parameter	Accuracy
LDA	Default	0.9758
SVM (Tuned)	Linear	0.9744
SVM (Default)	RBF	0.9120

The comparable performance between LDA (97.58%) and Linear SVM (97.44%), together with the lower accuracy obtained by the RBF kernel, suggests that the proposed MVP-PCA preprocessing effectively reduces the complexity of the original CNN feature distribution. Since Linear SVM assumes

a linear decision boundary, its competitive performance indicates that the transformed feature space has become sufficiently organized for linear classification without requiring nonlinear kernel mapping.

Figure 4 further supports this observation by showing that the decision boundary produced by the linear classifier separates the two classes with only limited overlap. This behavior indicates that MVP does not simply compress the feature space but also improves the spatial organization of class distributions before PCA projection.

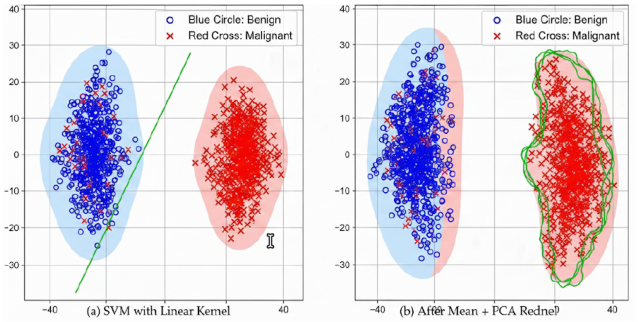

Figure 4. SVM decision boundaries on the MVP-PCA feature space, showing superior linear separability with the linear kernel.

Similarly, the t-SNE visualization in Figure 5 reveals more compact intra-class clusters and greater inter-class separation after MVP-PCA transformation. Although t-SNE serves only as a visualization technique rather than a quantitative evaluation, the observed cluster organization is consistent with the superior performance achieved by the linear classifiers, suggesting that the proposed preprocessing reduces irrelevant feature variance while preserving discriminative information.

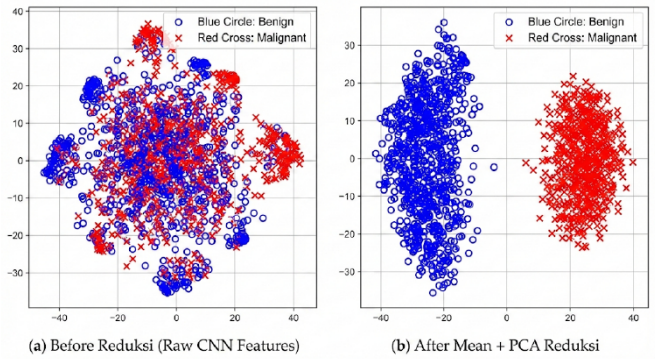

Figure 5. t-SNE visualization showing improved cluster separation after MVP-PCA transformation.

3.5. Clinical Impact and Error Analysis

the context of breast cancer detection, the sensitivity of the model, specifically the ability to minimize False Negatives (FN), is the most critical metric for patient safety. The detailed diagnostic outcomes for the best-performing configuration (Pipeline 1: MVP-PCA + LDA) are captured in the confusion matrix shown in (Figure 6).

The model successfully identified 145 true benign cases and 98 true malignant cases while producing only two false negatives, indicating that most malignant lesions were correctly recognized. he remaining false-negative cases may correspond to malignant lesions with imaging characteristics that closely resemble benign tissue, resulting in overlapping feature representations even after MVP-PCA transformation. In addition, subtle lesion characteristics may contribute only a small proportion of the overall feature variance and therefore become less prominent after dimensionality reduction. While 6 False Positive cases were recorded, this is clinically acceptable as it favors further diagnostic verification

over a missed diagnosis.

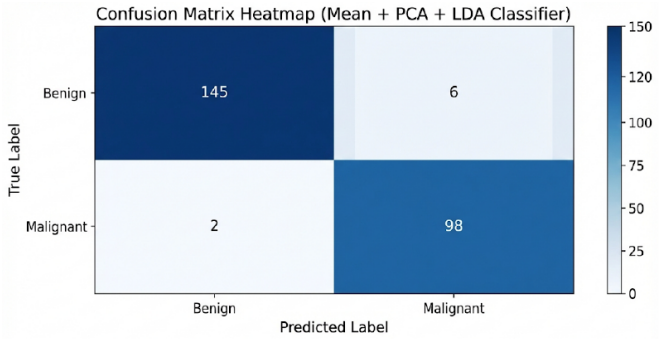

Figure 6. Confusion matrix of the proposed P1 architecture, showing high sensitivity with only 2 false negatives.

Despite the promising results, this study has several limitations. First, the proposed framework was evaluated using only a single public mammography dataset without external validation. Although the cross-validation results demonstrate good robustness, the generalizability of the proposed MVP-PCA framework across different imaging protocols, acquisition devices, and patient populations remains to be further investigated. Future studies should validate the proposed approach on multiple independent datasets to better assess its clinical applicability and robustness.

Second, this study focuses on comparing the proposed MVP-PCA framework with conventional PCA and LDA pipelines, while comparisons with more recent dimensionality reduction techniques, such as Kernel PCA, UMAP, or deep feature compression methods, have not yet been conducted. Furthermore, the current framework is limited to binary breast cancer classification. Future work will include broader benchmarking against state-of-the-art dimensionality reduction methods and extend the framework to multi-class breast cancer classification, including different malignancy grades, to evaluate its effectiveness in more clinically realistic scenarios.

4. Conclusion

This study demonstrates that conditioning the feature space before dimensionality reduction can substantially improve the effectiveness of conventional linear projection for breast cancer classification. By integrating Mean Vector Projection (MVP) with Principal Component Analysis (PCA), the proposed framework reduces irrelevant feature variance and improves the statistical organization of deep features extracted by SqueezeNet, enabling PCA to preserve more discriminative information without introducing additional trainable parameters or computationally intensive nonlinear transformations.

Experimental results show that the proposed MVP-PCA framework consistently outperforms the conventional PCA pipeline, achieving a classification accuracy of 97.58% while compressing the original feature representation by 99.11% into only 2,355 principal components. The comparable performance between linear classifiers and the observed reduction in cross-validation variability further suggest that feature conditioning before covariance-based projection improves the stability and separability of the transformed feature space. These findings indicate that the proposed framework provides an efficient and sustainable alternative for resource-constrained medical image analysis

Future research should validate the proposed framework on multiple independent breast cancer datasets and benchmark its performance against recent dimensionality reduction techniques, such as Kernel PCA, UMAP, and deep feature compression methods, to further evaluate its generalizability and computational efficiency. In addition, extending the framework to multi-class breast cancer classification involving different malignancy grades would provide a more comprehensive assessment of its clinical applicability.

Declaration of AI and AI assisted technologies in the writing process

During the preparation of this work, the authors used ChatGPT (OpenAI) to assist with improving the English language, grammar, sentence structure, and readability of the manuscript. The use of this tool was limited to language and writing assistance and did not replace the authors' intellectual contributions, research design, data analysis, interpretation, or scientific conclusions. After using this tool, the authors carefully reviewed and edited the content as needed and take full responsibility for the accuracy, originality, and integrity of the content of the published article.

Declaration of Competing Interest

The authors declare that they have no known competing financial interests or personal relationships that could have appeared to influence the work reported in this paper.

Acknowledgements

The authors would like to express their sincere gratitude to Universitas Dian Nuswantoro (UDINUS) and the IDSS Expertise Group in Smart Society, Food, and Agriculture for their valuable support, facilities, and contributions during the implementation and completion of this research. The authors also gratefully acknowledge all parties who provided assistance and support throughout the research process.

References

[1] A. A. S. Mohammad *et al.*, "Electronic Health Records Adoption: A Bibliometric Analysis," in *Intelligence-Driven Circular Economy*, vol. 1173, A. Hannoon and A. Mahmood, Eds., in Studies in Computational Intelligence, vol. 1173. , Cham: Springer Nature Switzerland, 2025, pp. 301–314. doi: https://doi.org/10.1007/978-3-031-73899-9_24.

[2] C. Eun-Mee, "Global trends in healthcare IT: EMR's central role and google trends insights," *J. Wellbeing Manag. Appl. Psychol.*, vol. 8, no. 1, pp. 43–53, 2025, doi: https://doi.org/10.13106/jwmap.2025.Vol8.no1.4344

[3] J. Huang *et al.*, "Acceptability, benefits and barriers of electronic health record radiology image sharing: A mixed-method study," *J. Med. Radiat. Sci.*, vol. 72, no. 2, pp. 244–254, Jun. 2025, doi: https://doi.org/10.1002/jmrs.853.

[4] T. Shiang *et al.*, "Inpatient Imaging Utilization and Radiology Workload: Trends of the Past Decade and Through the COVID-19 Pandemic," *J. Am. Coll. Radiol.*, vol. 22, no. 9, pp. 979–989, Sep. 2025, doi: https://doi.org/10.1016/j.jacr.2025.05.011.

[5] W. Bidgood Jr and S. C. Horii, "Introduction to the ACR-NEMA DICOM standard.," *Radiographics*, vol. 12, no. 2, pp. 345–355, 1992, doi: https://doi.org/10.1148/radiographics.12.2.1561424.

[6] J. S. Torres, J. Damian Segrelles Quilis, I. B. Espert, and V. H. García, "Improving knowledge management through the support of image examination and data annotation using DICOM structured reporting," *J. Biomed. Inform.*, vol. 45, no. 6, pp. 1066–1074, Dec. 2012, doi: https://doi.org/10.1016/j.jbi.2012.07.004.

[7] M. Y. Shakor and M. I. Khaleel, "Recent Advances in Big Medical Image Data Analysis Through Deep Learning and Cloud Computing," *Electronics*, vol. 13, no. 24, p. 4860, Dec. 2024, doi: https://doi.org/10.3390/electronics13244860.

[8] A. W. Salehi *et al.*, "A Study of CNN and Transfer Learning in Medical Imaging: Advantages, Challenges, Future Scope," *Sustainability*, vol. 15, no. 7, p. 5930, Mar. 2023, doi: https://doi.org/10.3390/su15075930.

[9] N. Cui, Y. Wu, G. Xin, J. Wu, L. Zhong, and H. Liang, "Application of Quantitative Interpretability to Evaluate CNN-Based Models for Medical Image Classification," *IEEE Access*, vol. 13, pp. 89386–89398, 2025, doi: https://doi.org/10.1109/ACCESS.2025.3567775.

[10] S. Iqbal, A. N. Qureshi, M. Alhussein, I. A. Choudhry, K. Aurangzeb, and T. M. Khan, "Fusion of Textural and Visual Information for Medical Image Modality Retrieval Using Deep Learning-

Based Feature Engineering," *IEEE Access*, vol. 11, pp. 93238–93253, 2023, doi: https://doi.org/10.1109/ACCESS.2023.3310245.
[11] C. Arizmendi, J. Pinto, A. Arboleda, and H. González, "Diagnosis of Patients with Viral, Bacterial, and Non-Pneumonia Based on Chest X-Ray Images Using Convolutional Neural Networks," *Int. J. Online Biomed. Eng. IJOE*, vol. 20, no. 16, pp. 52–65, Dec. 2024, doi: https://doi.org/10.3991/ijoe.v20i16.52895.
[12] V. Berisha *et al.*, "Digital medicine and the curse of dimensionality," *Npj Digit. Med.*, vol. 4, no. 1, p. 153, Oct. 2021, doi: https://doi.org/10.1038/s41746-021-00521-5.
[13] F. Ponzio, G. Urgese, E. Ficarra, and S. Di Cataldo, "Dealing with Lack of Training Data for Convolutional Neural Networks: The Case of Digital Pathology," *Electronics*, vol. 8, no. 3, p. 256, Feb. 2019, doi: https://doi.org/10.3390/electronics8030256.
[14] H. Rahman, A. R. Khan, T. Sadiq, A. H. Farooqi, I. U. Khan, and W. H. Lim, "A Systematic Literature Review of 3D Deep Learning Techniques in Computed Tomography Reconstruction," *Tomography*, vol. 9, no. 6, pp. 2158–2189, Dec. 2023, doi: https://doi.org/10.3390/tomography9060169.
[15] N. Tajbakhsh *et al.*, "Convolutional neural networks for medical image analysis: Full training or fine tuning?," *IEEE Trans. Med. Imaging*, vol. 35, no. 5, pp. 1299–1312, 2016, doi: https://doi.org/10.1109/TMI.2016.2535302
[16] F. Bargagna *et al.*, "Bayesian Convolutional Neural Networks in Medical Imaging Classification: A Promising Solution for Deep Learning Limits in Data Scarcity Scenarios," *J. Digit. Imaging*, vol. 36, no. 6, pp. 2567–2577, Dec. 2023, doi: https://doi.org/10.1007/s10278-023-00897-8.
[17] M. Woodland *et al.*, "Dimensionality Reduction for Improving Out-of-Distribution Detection in Medical Image Segmentation," in *Uncertainty for Safe Utilization of Machine Learning in Medical Imaging*, vol. 14291, C. H. Sudre, C. F. Baumgartner, A. Dalca, R. Mehta, C. Qin, and W. M. Wells, Eds., in Lecture Notes in Computer Science, vol. 14291. , Cham: Springer Nature Switzerland, 2023, pp. 147–156. doi: https://doi.org/10.1007/978-3-031-44336-7_15.
[18] A. K. Gárate-Escamila, A. Hajjam El Hassani, and E. Andrès, "Classification models for heart disease prediction using feature selection and PCA," *Inform. Med. Unlocked*, vol. 19, p. 100330, 2020, doi: https://doi.org/10.1016/j.imu.2020.100330.
[19] R. Massafra *et al.*, "Radiomic Feature Reduction Approach to Predict Breast Cancer by Contrast-Enhanced Spectral Mammography Images," *Diagnostics*, vol. 11, no. 4, p. 684, Apr. 2021, doi: https://doi.org/10.3390/diagnostics11040684.
[20] M. O. Adebiyi, M. O. Arowolo, M. D. Mshelia, and O. O. Olugbara, "A Linear Discriminant Analysis and Classification Model for Breast Cancer Diagnosis," *Appl. Sci.*, vol. 12, no. 22, p. 11455, Nov. 2022, doi: https://doi.org/10.3390/app122211455.
[21] A. H. KiRaz, F. O. Djibrillah, and M. E. Yüksel, "Deep feature extraction, dimensionality reduction, and classification of medical images using combined deep learning architectures, autoencoder, and multiple machine learning models," *Turk. J. Electr. Eng. Comput. Sci.*, vol. 31, no. 6, pp. 1113–1128, Oct. 2023, doi: https://doi.org/10.55730/1300-0632.4037.
[22] E. A. M. Stanley, R. Souza, M. Wilms, and N. D. Forkert, "Where, why, and how is bias learned in medical image analysis models? A study of bias encoding within convolutional networks using synthetic data," *eBioMedicine*, vol. 111, p. 105501, Jan. 2025, doi: https://doi.org/10.1016/j.ebiom.2024.105501.
[23] A. K. Pani, "Non-linear process monitoring using kernel principal component analysis: A review of the basic and modified techniques with industrial applications," *Braz. J. Chem. Eng.*, vol. 39, no. 2, pp. 327–344, 2022, doi: https://doi.org/10.1007/s43153-021-00125-2
[24] A. A. Wani, "Comprehensive review of dimensionality reduction algorithms: challenges, limitations, and innovative solutions," *PeerJ Comput. Sci.*, vol. 11, p. e3025, 2025, doi: https://doi.org/10.7717/peerj-cs.3025
[25] F. Song, Y. Sun, and G. Yuan, "Autonomous identification of bridge concrete cracks using unmanned aircraft images and improved lightweight deep convolutional networks," *Struct.*

Control Health Monit., vol. 2024, no. 1, p. 7857012, 2024, doi: https://doi.org/10.1155/2024/7857012
[26] F. N. Iandola, S. Han, M. W. Moskewicz, K. Ashraf, W. J. Dally, and K. Keutzer, "SqueezeNet: AlexNet-level accuracy with 50x fewer parameters and <0.5MB model size," Nov. 04, 2016, *arXiv*: arXiv:1602.07360. doi: https://doi.org/10.48550/arXiv.1602.07360.
[27] C. Carr *et al.*, "RSNA Screening Mammography Breast Cancer Detection." 2022. [Online]. Available: https://kaggle.com/competitions/rsna-breast-cancer-detection
[28] Z. Khodabandeh *et al.*, "Discrimination of multiple sclerosis using OCT images from two different centers," *Mult. Scler. Relat. Disord.*, vol. 77, p. 104846, Sep. 2023, doi: https://doi.org/10.1016/j.msard.2023.104846.
[29] H. Avcı and J. Karakaya, "A Novel Medical Image Enhancement Algorithm for Breast Cancer Detection on Mammography Images Using Machine Learning," *Diagnostics*, vol. 13, no. 3, p. 348, Jan. 2023, doi: https://doi.org/10.3390/diagnostics13030348.
[30] C. M. Bishop and N. M. Nasrabadi, *Pattern recognition and machine learning*, vol. 4. Springer, 2006.
[31] I. T. Jolliffe, *Principal Component Analysis*. in Springer Series in Statistics. Springer New York, 2002. [Online]. Available: https://books.google.co.id/books?id=-ongBwAAQBAJ doi: https://doi.org/10.1007/b98835
[32] D. G. Stork, R. O. Duda, and P. E. Hart, *Pattern classification*. John Wiley., 2001.
[33] T. Hastie, R. Tibshirani, J. Friedman, and others, "The elements of statistical learning." Springer series in statistics New-York, 2009. doi: https://doi.org/10.1007/978-0-387-84858-7
[34] C. Cortes and V. Vapnik, "Support-vector networks," *Mach. Learn.*, vol. 20, no. 3, pp. 273–297, 1995. doi: https://doi.org/10.1007/BF00994018
[35] D. S. Mouliou and K. I. Gourgoulianis, "False-positive and false-negative COVID-19 cases: respiratory prevention and management strategies, vaccination, and further perspectives," *Expert Rev. Respir. Med.*, vol. 15, no. 8, pp. 993–1002, Aug. 2021, doi: https://doi.org/10.1080/17476348.2021.1917389.